

# Nuclear deformation and neutrinoless double- $\beta$ decay of $^{94,96}\text{Zr}$ , $^{98,100}\text{Mo}$ , $^{104}\text{Ru}$ , $^{110}\text{Pd}$ , $^{128,130}\text{Te}$ and $^{150}\text{Nd}$ nuclei in mass mechanism

K. Chaturvedi<sup>1,2</sup>, R. Chandra<sup>1,3</sup>, P. K. Rath<sup>1</sup>, P. K. Raina<sup>3</sup> and J. G. Hirsch<sup>4</sup>

<sup>1</sup>*Department of Physics, University of Lucknow, Lucknow-226007, India*

<sup>2</sup>*Department of Physics, Bundelkhand University, Jhansi-284128, India*

<sup>3</sup>*Department of Physics and Meteorology, IIT Kharagpur-721302, India*

<sup>4</sup>*Instituto de Ciencias Nucleares, Universidad Nacional Autónoma de México, A.P. 70-543, México 04510 D.F., México*

(Dated: October 28, 2018)

The  $(\beta^-\beta^-)_{0\nu}$  decay of  $^{94,96}\text{Zr}$ ,  $^{98,100}\text{Mo}$ ,  $^{104}\text{Ru}$ ,  $^{110}\text{Pd}$ ,  $^{128,130}\text{Te}$  and  $^{150}\text{Nd}$  isotopes for the  $0^+ \rightarrow 0^+$  transition is studied in the Projected Hartree-Fock-Bogoliubov framework. In our earlier work, the reliability of HFB intrinsic wave functions participating in the  $\beta^-\beta^-$  decay of the above mentioned nuclei has been established by obtaining an overall agreement between the theoretically calculated spectroscopic properties, namely yrast spectra, reduced  $B(E2:0^+ \rightarrow 2^+)$  transition probabilities, quadrupole moments  $Q(2^+)$ , gyromagnetic factors  $g(2^+)$  as well as half-lives  $T_{1/2}^{2\nu}$  for the  $0^+ \rightarrow 0^+$  transition and the available experimental data. In the present work, we study the  $(\beta^-\beta^-)_{0\nu}$  decay for the  $0^+ \rightarrow 0^+$  transition in the mass mechanism and extract limits on effective mass of light as well as heavy neutrinos from the observed half-lives  $T_{1/2}^{0\nu}(0^+ \rightarrow 0^+)$  using nuclear transition matrix elements calculated with the same set of wave functions. Further, the effect of deformation on the nuclear transition matrix elements required to study the  $(\beta^-\beta^-)_{0\nu}$  decay in the mass mechanism is investigated. It is noticed that the deformation effect on nuclear transition matrix elements is of approximately same magnitude in  $(\beta^-\beta^-)_{2\nu}$  and  $(\beta^-\beta^-)_{0\nu}$  decay.

PACS numbers: 23.40.Bw, 23.40.Hc, 21.60.Jz, 27.60.+j, 27.70.+q

## I. INTRODUCTION

The experimental search for mass and nature of neutrinos through terrestrial as well as extra-terrestrial approaches has finally confirmed the neutrino oscillation in atmospheric [1, 2, 3], solar [4, 5, 6], reactor [7, 8] and accelerator [9, 10] neutrino sources and it has been established that neutrinos have mass. Further, it is generally agreed that oscillations among three neutrino species are sufficient to explain the atmospheric, solar, reactor and accelerator neutrino puzzle. The neutrino oscillation experiments provide us with neutrino mass square differences  $\Delta m^2$ , mixing angles and possible hierarchy in the neutrino mass spectrum. The global analysis of atmospheric, solar, reactor (Kam-LAND and CHOOZ) and accelerator (K2K and MINOS) neutrino oscillation data with  $2\sigma$  ( $3\sigma$ ) error provides  $\Delta m_{12}^2 = 7.6_{-0.3}^{+0.5} \times 10^{-5}$  ( $7.6_{-0.5}^{+0.7} \times 10^{-5}$ ) eV<sup>2</sup>,  $\sin^2\theta_{12} = 0.32_{-0.4}^{+0.5}$  ( $0.32_{-0.6}^{+0.8}$ ) for solar neutrinos,  $\Delta m_{23}^2 = 2.4 \pm 0.3 \times 10^{-3}$  ( $2.4 \pm 0.4 \times 10^{-3}$ ) eV<sup>2</sup>,  $\sin^2\theta_{23} = 0.50_{-0.12}^{+0.13}$  ( $0.50_{-0.16}^{+0.17}$ ) for atmospheric neutrinos and  $\sin^2\theta_{13} \leq 0.033$  (0.050) [11]. The oscillation data also suggest that the neutrinos may belong to either normal hierarchy ( $m_1 < m_2 < m_3$ ) or inverted hierarchy ( $m_3 < m_1 < m_2$ ). The data do not exclude the possibility that the mass of the light neutrino is much larger than  $\sqrt{\Delta m_a^2}$  and this implies the possible existence of quasi-degenerate neutrino mass spectrum i.e.  $m_1 \simeq m_2 \simeq m_3$ . However, the actual mass of neutrinos cannot be extracted from these data. On the other hand, the study of tritium single  $\beta$ -decay and nuclear double- $\beta$  ( $\beta\beta$ ) decay together can provide sharpest limits on the mass and nature of neutrinos.

The nuclear  $\beta\beta$  decay is a rare second order semi-leptonic transition between two even  $Z$ -even  $N$  isobars  ${}^A_Z X$  and  ${}^A_{Z\pm 2} Y$  involving strangeness conserving charged weak currents. The implications of present studies about nuclear  $\beta\beta$  decay, which is expected to proceed through four experimentally distinguishable modes, namely the two neutrino double beta ( $\beta\beta$ )<sub>2 $\nu$</sub>  decay, neutrinoless double beta ( $\beta\beta$ )<sub>0 $\nu$</sub>  decay, single Majoron accompanied ( $\beta\beta\phi$ )<sub>0 $\nu$</sub>  decay and double Majoron accompanied ( $\beta\beta\phi\phi$ )<sub>0 $\nu$</sub>  decay are far reaching in nature. The half-life of ( $\beta\beta$ )<sub>2 $\nu$</sub>  decay is a product of accurately known phase space factor and appropriate nuclear transition matrix element (NTME)  $M_{2\nu}$ . It has been already measured in the case of  $(\beta^-\beta^-)_{2\nu}$  decay for about ten nuclei out of 35 possible candidates [12]. Hence, the values of NTMEs  $M_{2\nu}$  can be extracted directly. Consequently, the validity of different models employed for nuclear structure calculations can be tested by calculating the  $M_{2\nu}$ . The ( $\beta\beta$ )<sub>0 $\nu$</sub>  decay, which violates the conservation of lepton number, can occur in a number of gauge theoretical models, namely GUTs -left-right symmetric models and E(6)-,  $R_p$ -conserving as well as violating SUSY models, in the scenarios of leptoquark exchange, existence of heavy sterile neutrino, compositeness and Majoron models. Hence, it is a convenient tool to test the physics beyond the standard model (SM). In particular for the question whether the neutrino is a Majorana or Dirac particle, the ( $\beta\beta$ )<sub>0 $\nu$</sub>  decay is considered to be the most sensitive way of distinguishing between these two possibilities. The experimental as well as theoretical developments in the study of nuclear  $\beta\beta$  decay have been excellently reviewed over the past

years [13, 14, 15, 16, 17, 18, 19, 20, 21, 22, 23, 24, 25, 26, 27, 28, 29, 30, 31, 32].

The  $(\beta^-\beta^-)_{0\nu}$  decay has not been observed so far and the best observed limit on half-life  $T_{1/2}^{0\nu} > 1.9 \times 10^{25}$  yr for  $^{76}\text{Ge}$  has been achieved in the Heidelberg-Moscow experiment [33]. Klapdor and his group have recently reported that  $(\beta^-\beta^-)_{0\nu}$  decay has been observed in  $^{76}\text{Ge}$  and  $T_{1/2}^{0\nu} = 1.19 \times 10^{25}$  yr [34]. However, it is felt that the latter result needs independent verification [28, 35, 36]. The aim of all the present experimental activities is to observe the  $(\beta^-\beta^-)_{0\nu}$  decay. Hence, the models predict half-lives assuming certain value for the neutrino mass or conversely extract various parameters from the observed limits of the half-lives of  $(\beta\beta)_{0\nu}$  decay. The reliability of predictions can be judged a priori only from the success of a nuclear model in explaining various observed physical properties of nuclei. The common practice is to calculate the  $M_{2\nu}$  to start with and compare them with the experimentally observed value as the two decay modes involve the same set of initial and final nuclear wave functions although the structure of nuclear transition operators are quite different. Over the past few years, the  $(\beta\beta)_{0\nu}$  decay has been studied mainly in three types of models, namely shell model and its variants, the quasiparticle random phase approximation (QRPA) and its extensions and alternative models. In the recent past, the advantages as well as shortcomings of these models have been excellently discussed by Suhonen *et al.* [21] and Faessler *et al.* [22].

The structure of nuclei in the mass region  $94 \leq A \leq 150$  is quite complex. In the mass region  $A \approx 100$ , the reduced  $B(E2:0^+ \rightarrow 2^+)$  transition probabilities of Zr, Mo, Ru, Pd and Cd isotopes were observed to be as enhanced as in the rare-earth and actinide regions. This mass region offers a nice example of shape transition through sudden onset of deformation at neutron number  $N = 60$ . The nuclei are soft vibrators for neutron number  $N < 60$  and quasi-rotors for  $N > 60$ . The nuclei with neutron number  $N = 60$  are transitional nuclei. Similarly, the Te and Xe isotopes in the mass region  $A \approx 130$  have a vibrational and rotational excitation spectra respectively. The mass region  $A \approx 150$  offers another example of shape transition i.e. the sudden onset of deformation at neutron number  $N = 90$ . Nuclei range from spherical to well deformed, with large static quadrupole moments. In the mass region  $94 \leq A \leq 150$  of our interest, the experimental deformation parameter  $\beta_2$  varies from  $0.081 \pm 0.016$  to  $0.2848 \pm 0.0021$  [37]. The lowest and highest  $\beta_2$  values correspond to  $^{96}\text{Zr}$  and  $^{150}\text{Nd}$  respectively. It is well known that the pairing part of the interaction ( $P$ ) accounts for the sphericity of nucleus, whereas the quadrupole-quadrupole ( $QQ$ ) interaction increases the collectivity in the nuclear intrinsic wave functions and makes the nucleus deformed. Hence, it is expected that subtle interplay of pairing and deformation degrees of freedom will play a crucial role in reproducing the properties of nuclei in this mass region. All the nuclei undergoing  $\beta\beta$  decay are even-even type, in which the pairing degrees of freedom play an important role. Moreover, it has been already conjectured that the deformation can play a crucial role in case of  $\beta^-\beta^-$  decay of  $^{100}\text{Mo}$  and  $^{150}\text{Nd}$  isotopes [38, 39]. Hence, it is desirable to have a model which incorporates the pairing and deformation degrees of freedom on equal footing in its formalism.

In the light of above discussions, the PHFB model is one of the most natural choices. However, it is not possible to study the structure of odd-odd nuclei in the present version of the PHFB model. Hence, the single  $\beta$ -decay rates and the distribution of Gamow-Teller strength can not be calculated. On the other hand, the study of these processes has implications in the understanding of the role of the isoscalar part of the proton-neutron interaction. This is a serious draw back in the present formalism of the PHFB model. Notwithstanding, the PHFB model in conjunction with the summation method has been successfully applied to the  $(\beta^-\beta^-)_{2\nu}$  decay of  $^{94,96}\text{Zr}$ ,  $^{98,100}\text{Mo}$ ,  $^{104}\text{Ru}$  and  $^{110}\text{Pd}$  [40],  $^{128,130}\text{Te}$  and  $^{150}\text{Nd}$  [41] isotopes for the  $0^+ \rightarrow 0^+$  transition not in isolation but together with other observed nuclear spectroscopic properties, namely yrast spectra, reduced  $B(E2)$  transition probabilities, static quadrupole moments and  $g$ -factors. The success of the PHFB model in conjunction with the  $PPQQ$  interaction in explaining  $(\beta^-\beta^-)_{2\nu}$  decay as well as the above mentioned nuclear properties in the mass range  $94 \leq A \leq 150$  has prompted us to apply the same to study the  $(\beta^-\beta^-)_{0\nu}$  decay of the same nuclei for the  $0^+ \rightarrow 0^+$  transition. Further, the PHFB model using the  $PPQQ$  interaction is a convenient choice to examine the explicit role of deformation on NTMEs  $M_{2\nu}$ . In the case of  $(\beta^-\beta^-)_{2\nu}$  decay, we have observed that the deformation plays an important role in the quenching of  $M_{2\nu}$  by a factor of approximately 2 to 6 [40, 41]. Therefore, we also study the variation of NTMEs of  $(\beta^-\beta^-)_{0\nu}$  decay vis-a-vis the change in deformation through the changing strength of the  $QQ$  interaction.

Our aim is to extract limits on the effective mass of light as well as heavy neutrinos from the study of the  $(\beta^-\beta^-)_{0\nu}$  decay of  $^{94,96}\text{Zr}$ ,  $^{98,100}\text{Mo}$ ,  $^{104}\text{Ru}$ ,  $^{110}\text{Pd}$ ,  $^{128,130}\text{Te}$  and  $^{150}\text{Nd}$  isotopes for the  $0^+ \rightarrow 0^+$  transition. The present paper is organized as follows. The theoretical formalism to calculate the half-life of the  $(\beta\beta)_{0\nu}$  decay mode has been given by Vergados [15] and Doi *et al.* [19]. Hence, we briefly outline steps of the above derivations in Sec. II for clarity in notations used in the present paper following Doi *et al.* [19]. In Sec. III, we present the results and discuss them vis-a-vis the existing calculations done in other nuclear models. The deformation effect on NTMEs of  $(\beta^-\beta^-)_{0\nu}$  decay in the mass mechanism is also discussed in the same Section. Finally, the conclusions are given in Sec. IV.

## II. THEORETICAL FORMALISM

The effective weak interaction Hamiltonian density for  $\beta^-$ -decay due to  $W$ -boson exchange restricted to left-handed currents, is given by

$$H_W = \frac{G}{\sqrt{2}} j_{L\mu} J_L^{\mu\dagger} + h.c. \quad (1)$$

where

$$\frac{G}{\sqrt{2}} = \frac{g^2}{8M_1^2} \left[ \cos^2 \zeta + \left( \frac{M_1}{M_2} \right)^2 \sin^2 \zeta \right] \quad (2)$$

The gauge bosons  $W_L$  and  $W_R$  are the superposition of mass eigenstates  $W_1$  and  $W_2$  with masses  $M_1$  and  $M_2$  respectively and mixing angle  $\zeta$ , and  $G = 1.16637 \times 10^{-5} \text{ GeV}^{-2}$ . The left handed  $V - A$  weak leptonic charged current is given by

$$j_{L\mu} = \bar{e} \gamma_\mu (1 - \gamma_5) \nu_{eL} \quad (3)$$

where

$$\nu_{eL} = \sum_{i=1}^{2n} U_{ei} N_{iL} \quad (4)$$

Here,  $N_i$  is a Majorana neutrino field with mass  $m_i$ . In Eq. (4), a Dirac neutrino is expressed as a superposition of a pair of mass degenerate Majorana neutrinos in the most general form. Further, the mixing parameters are constrained by the following orthonormality conditions.

$$\sum_{i=1}^{2n} |U_{ei}|^2 = \sum_{i=1}^{2n} |V_{ei}|^2 = 1 \quad \text{and} \quad \sum_{i=1}^{2n} U_{ei} V_{ei} = 0 \quad (5)$$

The strangeness conserving  $V - A$  hadronic currents are given by

$$J_L^{\mu\dagger} = g_V \bar{u} \gamma^\mu (1 - \gamma_5) d \quad (6)$$

where

$$g_V = \cos \theta_c \quad (7)$$

In Eq. (7), the  $\theta_c$  is the Cabibbo-Kobayashi-Maskawa (CKM) mixing angle for the left handed  $d$  and  $s$  quarks.

In the mass mechanism, the following approximations are taken in deriving the half-life of  $(\beta^- \beta^-)_{0\nu}$  decay.

- (i) The light neutrino species of mass  $m_i < 10 \text{ MeV}$  and heavy neutrinos of mass  $m_i > 1 \text{ GeV}$  are considered.
- (ii) In the  $0^+ \rightarrow 0^+$  transition, the  $s_{1/2}$  waves are considered to describe the final leptonic states.
- (iii) The nonrelativistic impulse approximation is considered for the hadronic currents.
- (iv) The tensorial terms in the hadronic currents [42] are neglected. While according to Ref. [43] they can reduce the matrix elements up to 30%, in Ref. [44] it was reported that its contribution is quite small and can be safely neglected.
- (v) In the case of  $(\beta^- \beta^-)_{0\nu}$  decay, the exchanged neutrinos are virtual particles. Their typical energy  $\omega = (q^2 + m^2)^{1/2}$  is much larger than the typical excitation energy of the intermediate nuclear states

$$\omega \sim 100 \text{ MeV} \gg E_N - E_I \sim k^2/M \sim 10 \text{ MeV} \quad (8)$$

and the variation of  $E_N$  in the energy denominator can be safely neglected. Hence, the closure approximation is valid and it is usually used by replacing the  $E_N$  by an average  $\langle E_N \rangle$ .

(vi) No finite de Broglie wave length correction is considered. This assumption helps in the calculation of phase space factors.

(vii) The CP conservation is assumed so that the  $U_{ei}$  and  $V_{ei}$  are both real or purely imaginary depending on the CP parity of the mass eigenstates of neutrinos  $N$  and consequently the effective neutrino masses  $\langle m_\nu \rangle$  and  $\langle M_N \rangle$  for the light and heavy neutrinos are real.

In mass mechanism, the inverse half-life of  $(\beta^-\beta^-)_{0\nu}$  decay in 2n mechanism for the  $0^+ \rightarrow 0^+$  transition is given by [15, 19]

$$\begin{aligned} [T_{1/2}^{0\nu}(0^+ \rightarrow 0^+)]^{-1} &= \left(\frac{\langle m_\nu \rangle}{m_e}\right)^2 G_{01} (M_{GT} - M_F)^2 + \left(\frac{m_p}{\langle M_N \rangle}\right)^2 G_{01} (M_{GT_h} - M_{F_h})^2 \\ &+ \left(\frac{\langle m_\nu \rangle}{m_e}\right) \left(\frac{m_p}{\langle M_N \rangle}\right) G_{01} (M_{GT} - M_F) (M_{GT_h} - M_{F_h}) \end{aligned} \quad (9)$$

where

$$\langle m_\nu \rangle = \sum_i' U_{ei}^2 m_i, \quad m_i < 10\text{MeV}, \quad (10)$$

$$\langle M_N \rangle^{-1} = \sum_i'' U_{ei}^2 m_i^{-1}, \quad m_i > 1\text{GeV} \quad (11)$$

In the closure approximation, NTMEs  $M_\alpha$  are written as

$$M_\alpha = \sum_{n,m} \langle 0_F^+ || O_{\alpha,nm} \tau_n^+ \tau_m^+ || 0_I^+ \rangle \quad (12)$$

where the nuclear transition operators are given by

$$O_F = \left(\frac{g_V}{g_A}\right)^2 H_m(r) \quad (13)$$

$$O_{GT} = \sigma_1 \cdot \sigma_2 H_m(r) \quad (14)$$

$$O_{F_h} = 4\pi (M_p m_e)^{-1} \left(\frac{g_V}{g_A}\right)^2 \delta(\mathbf{r}) \quad (15)$$

$$O_{GT_h} = 4\pi (M_p m_e)^{-1} \sigma_1 \cdot \sigma_2 \delta(\mathbf{r}) \quad (16)$$

The neutrino potentials  $H_m(r)$  arising due to the exchange of light neutrinos is defined as

$$\begin{aligned} H_m(r) &= \frac{4\pi R}{(2\pi)^3} \int d^3q \frac{\exp(i\mathbf{q} \cdot \mathbf{r})}{\omega(\omega + \bar{A})} \\ &= \frac{2R}{\pi r} \int \frac{\sin(qr)}{(q + \bar{A})} dq \\ &= \frac{R}{r} \phi(\bar{A}r) \end{aligned} \quad (17)$$

In going from the first to second line of Eq. (17), the neutrino mass has been neglected in comparison with the typical neutrino momentum  $q \approx 200 m_e$ . Further

$$\bar{A} = \langle E_N \rangle - \frac{1}{2} (E_I + E_F) \quad (18)$$

The function  $\phi(x)$  is defined by

$$\phi(x) = \frac{2}{\pi} (\sin x \text{ci}(x) - \cos x \text{si}(x)) \quad (19)$$

where

$$\text{ci}(x) = - \int_x^\infty t^{-1} \cos t dt \quad \text{and} \quad \text{si}(x) = - \int_x^\infty t^{-1} \sin t dt \quad (20)$$

In the PHFB model, the long range correlations are taken into account through the configuration mixing while the short range correlations due to the repulsive hard core is usually absent. In a microscopic picture, the short range correlations (SRC) arise mainly from the repulsive nucleon-nucleon potential arising due to the exchange of  $\rho$  and  $\omega$  mesons. Hirsch *et al.* have included the short range effects through the  $\omega$ -meson exchange to study the  $(\beta^-\beta^-)_{0\nu}$

decay in heavy deformed nuclei [45]. The effect due to SRC has been recently studied by Kortelainen *et al.* [46] and Simkovic *et al.* [56] in the unitary correlation operator method (UCOM). This SRC effect can also be incorporated phenomenologically by using the Jastrow type of correlation given by the prescription

$$\langle j_1^\pi j_2^\pi J | O | j_1^\nu j_2^\nu J' \rangle \rightarrow \langle j_1^\pi j_2^\pi J | f O f | j_1^\nu j_2^\nu J' \rangle \quad (21)$$

where

$$f(r) = 1 - e^{-ar^2}(1 - br^2) \quad (22)$$

with  $a = 1.1 \text{ fm}^{-2}$  and  $b = 0.68 \text{ fm}^{-2}$ . However, it is not clear which approach is the best [56]. Therefore, we include the short range correlation by using the Jastrow correlations given by Eq. (22) in the present work. Wu and co-workers [47] derived the effective transition operator  $\widehat{f}O\widehat{f}$  for the  $(\beta^-\beta^-)_{0\nu}$  decay of  $^{48}\text{Ca}$  using Reid and Paris potentials. The calculations show that phenomenologically determined  $f(r)$  has strong two nucleon correlations. The consideration of the effect due to SRC requires the inclusion of finite size of the nucleon and is taken into account by the replacements

$$g_V \rightarrow g_V \left( \frac{\Lambda^2}{\Lambda^2 + k^2} \right)^2 \quad \text{and} \quad g_A \rightarrow g_A \left( \frac{\Lambda^2}{\Lambda^2 + k^2} \right)^2 \quad (23)$$

with  $\Lambda = 850 \text{ MeV}$ . Including finite size effect, the neutrino potential for the exchange of heavy neutrinos  $U_0(r, \Lambda)$  is written as

$$\begin{aligned} U_0(r, \Lambda) &= \frac{R}{(2\pi)^3} \int d\mathbf{k} e^{i\mathbf{k}\cdot\mathbf{r}} \left( \frac{\Lambda^2}{\Lambda^2 + k^2} \right)^4 \\ &= \frac{R}{2\pi^2 r} \int \sin(qr) \left( \frac{\Lambda^2}{\Lambda^2 + k^2} \right)^4 q dq \end{aligned} \quad (24)$$

$$= \frac{\Lambda^3 R}{64\pi} e^{-\Lambda r} \left[ 1 + \Lambda r + \frac{1}{3} (\Lambda r)^2 \right] \quad (25)$$

The expression to calculate the NTMEs  $M_\alpha$  of  $(\beta^-\beta^-)_{0\nu}$  decay for the  $0^+ \rightarrow 0^+$  transition in the PHFB model is obtained as follows. In the PHFB model, a state with good angular momentum  $\mathbf{J}$  is obtained from the axially symmetric HFB intrinsic state  $|\Phi_0\rangle$  with  $K = 0$  through the following relation using the standard projection technique [48]

$$|\Psi_{00}^J\rangle = \left[ \frac{(2J+1)}{8\pi^2} \right] \int D_{00}^J(\Omega) R(\Omega) |\Phi_0\rangle d\Omega \quad (26)$$

where  $R(\Omega)$  and  $D_{MK}^J(\Omega)$  are the rotation operator and the rotation matrix respectively. The axially symmetric HFB intrinsic state  $|\Phi_0\rangle$  can be written as

$$|\Phi_0\rangle = \prod_{im} (u_{im} + v_{im} b_{im}^\dagger b_{i\bar{m}}^\dagger) |0\rangle \quad (27)$$

where the creation operators  $b_{im}^\dagger$  and  $b_{i\bar{m}}^\dagger$  are defined as

$$b_{im}^\dagger = \sum_\alpha C_{i\alpha, m} a_{\alpha m}^\dagger \quad \text{and} \quad b_{i\bar{m}}^\dagger = \sum_\alpha (-1)^{l+j-m} C_{i\alpha, m} a_{\alpha, -m}^\dagger \quad (28)$$

The amplitudes  $(u_{im}, v_{im})$  and the expansion coefficient  $C_{ij, m}$  are obtained from the HFB calculations.

Employing the HFB wave functions, one obtains the following expression for NTMEs  $M_\alpha$  of  $(\beta^-\beta^-)_{0\nu}$  decay [49].

$$\begin{aligned} M_\alpha &= [n^{J_i=0} n^{J_f=0}]^{-1/2} \int_0^\pi n_{(Z, N), (Z+2, N-2)}(\theta) \frac{1}{4} \sum_{\alpha\beta\gamma\delta} \langle \alpha\beta | O_\alpha | \gamma\delta \rangle \\ &\times \sum_{\varepsilon\eta} \frac{\left( f_{Z+2, N-2}^{(\pi)*} \right)_{\varepsilon\beta} \left( F_{Z, N}^{(\nu)*} \right)_{\eta\delta}}{\left[ \left( 1 + F_{Z, N}^{(\pi)}(\theta) f_{Z+2, N-2}^{(\pi)*} \right)_{\varepsilon\alpha} \right]^{-1} \left[ \left( 1 + F_{Z, N}^{(\nu)}(\theta) f_{Z+2, N-2}^{(\nu)*} \right)_{\gamma\eta} \right]^{-1}} \sin\theta d\theta \end{aligned} \quad (29)$$

where

$$n^J = \int_0^\pi \left[ \det \left( 1 + F^{(\pi)} f^{(\pi)\dagger} \right) \right]^{1/2} \left[ \det \left( 1 + F^{(\nu)} f^{(\nu)\dagger} \right) \right]^{1/2} d_{00}^J(\theta) \sin(\theta) d\theta \quad (30)$$

and

$$n_{(Z,N),(Z+2,N-2)}(\theta) = \left[ \det \left( 1 + F_{Z,N}^{(\nu)} f_{Z+2,N-2}^{(\nu)\dagger} \right) \right]^{1/2} \times \left[ \det \left( 1 + F_{Z,N}^{(\pi)} f_{Z+2,N-2}^{(\pi)\dagger} \right) \right]^{1/2} \quad (31)$$

The  $\pi(\nu)$  represents the proton (neutron) of nuclei involved in the  $(\beta\beta)_{0\nu}$  decay process. The matrix  $F_{Z,N}(\theta)$  and  $f_{Z,N}$  are given by

$$F_{Z,N}(\theta) = \sum_{m'_\alpha m'_\beta} d_{m_\alpha, m'_\alpha}^{j_\alpha}(\theta) d_{m_\beta, m'_\beta}^{j_\beta}(\theta) f_{j_\alpha m'_\alpha, j_\beta m'_\beta} \quad (32)$$

$$f_{Z,N} = \sum_i C_{ij_\alpha, m_\alpha} C_{ij_\beta, m_\beta} (v_{im_\alpha} / u_{im_\alpha}) \delta_{m_\alpha, -m_\beta} \quad (33)$$

The calculation of required NTMEs  $M_\alpha$  are performed in the following manner. In the first step, matrices  $f^{(\pi, \nu)}$  and  $F^{(\pi, \nu)}(\theta)$  are setup for the nuclei involved in the  $(\beta\beta)_{0\nu}$  decay making use of 20 Gaussian quadrature points in the range  $(0, \pi)$ . Finally, the required NTMEs can be calculated in a straight forward manner using the Eq. (29).

It is worth to underline the fact that the building blocks for constructing the HFB states are spherical harmonic oscillator states, which depend only on the mass number  $A$  and there is no dependence on  $N$  and  $Z$ . For this reason the overlap expressions given above are exact in the present context, and the ‘‘two vacua’’ problem found in QRPA calculations [50] is not present.

### III. RESULTS AND DISCUSSIONS

In the present work, we calculate the NTMEs  $M_F$ ,  $M_{GT}$ ,  $M_{Fh}$  and  $M_{GT_h}$  for  $^{94,96}\text{Zr}$ ,  $^{98,100}\text{Mo}$ ,  $^{104}\text{Ru}$ ,  $^{110}\text{Pd}$ ,  $^{128,130}\text{Te}$  and  $^{150}\text{Nd}$  isotopes to study the  $0^+ \rightarrow 0^+$  transition of  $(\beta^-\beta^-)_{0\nu}$  decay in the mass mechanism using a set of HFB wave functions, the reliability of which was tested by obtaining an over all agreement between theoretically calculated results for the yrast spectra, reduced  $B(E2:0^+ \rightarrow 2^+)$  transition probabilities, static quadrupole moments  $Q(2^+)$ ,  $g$ -factors  $g(2^+)$  and NTMEs  $M_{2\nu}$  as well as half-lives  $T_{1/2}^{2\nu}$  of  $(\beta^-\beta^-)_{2\nu}$  decay and the available experimental data [40, 41]. However, we briefly discuss in the following the model space, single particle energies (SPE's) and parameters of two-body interactions used to generate the HFB wave functions for convenience.

We treat the doubly even nucleus  $^{76}\text{Sr}$  ( $N = Z = 38$ ) as an inert core in case of  $^{94,96}\text{Zr}$ ,  $^{94,96,98,100}\text{Mo}$ ,  $^{98,100,104}\text{Ru}$ ,  $^{104,110}\text{Pd}$  and  $^{110}\text{Cd}$  nuclei, with the valence space spanned by  $1p_{1/2}$ ,  $2s_{1/2}$ ,  $1d_{3/2}$ ,  $1d_{5/2}$ ,  $0g_{7/2}$ ,  $0g_{9/2}$  and  $0h_{11/2}$  orbits for protons and neutrons. The  $1p_{1/2}$  orbit has been included in the valence space to examine the role of the  $Z = 40$  proton core vis-a-vis the onset of deformation in the highly neutron rich isotopes. The set of single particle energies (SPE's) used were (in MeV)  $\varepsilon(1p_{1/2}) = -0.8$ ,  $\varepsilon(0g_{9/2}) = 0.0$ ,  $\varepsilon(1d_{5/2}) = 5.4$ ,  $\varepsilon(2s_{1/2}) = 6.4$ ,  $\varepsilon(1d_{3/2}) = 7.9$ ,  $\varepsilon(0g_{7/2}) = 8.4$  and  $\varepsilon(0h_{11/2}) = 8.6$  for proton and neutron.

In case of  $^{128,130}\text{Te}$ ,  $^{128,130}\text{Xe}$ ,  $^{150}\text{Nd}$  and  $^{150}\text{Sm}$  nuclei, we treated the doubly even nucleus  $^{100}\text{Sn}$  ( $N = Z = 50$ ) as an inert core with the valence space spanned by  $2s_{1/2}$ ,  $1d_{3/2}$ ,  $1d_{5/2}$ ,  $1f_{7/2}$ ,  $0g_{7/2}$ ,  $0h_{9/2}$  and  $0h_{11/2}$  orbits for protons and neutrons. The change of model space was forced upon due to the following reason. In the model space used for mass region  $A \approx 100$ , the number of neutrons increase to about 40 for nuclei occurring in the mass region  $A \approx 130$ . With the increase in neutron number, the yrast energy spectra gets compressed due to increase in the attractive part of effective two-body interaction. The set of single particle energies (SPE's) used were in MeV:  $\varepsilon(1d_{5/2}) = 0.0$ ,  $\varepsilon(2s_{1/2}) = 1.4$ ,  $\varepsilon(1d_{3/2}) = 2.0$ ,  $\varepsilon(0g_{7/2}) = 4.0$ ,  $\varepsilon(0h_{11/2}) = 6.5$  (4.8 for  $^{150}\text{Nd}$  and  $^{150}\text{Sm}$ ),  $\varepsilon(1f_{7/2}) = 12.0$  (11.5 for  $^{150}\text{Nd}$  and  $^{150}\text{Sm}$ ),  $\varepsilon(0h_{9/2}) = 12.5$  (12.0 for  $^{150}\text{Nd}$  and  $^{150}\text{Sm}$ ) for proton and neutron.

The HFB wave functions were generated using an effective Hamiltonian with  $PPQQ$  type [51] of two-body interaction. Explicitly, the Hamiltonian can be written as

$$H = H_{sp} + V(P) + \zeta_{qq} V(QQ) \quad (34)$$

where  $H_{sp}$  denotes the single particle Hamiltonian. The  $V(P)$  and  $V(QQ)$  represent the pairing and quadrupole-quadrupole part of the effective two-body interaction. The  $\zeta_{qq}$  is an arbitrary parameter and the final results were obtained by setting the  $\zeta_{qq} = 1$ . The purpose of introducing  $\zeta_{qq}$  was to study the role of deformation by varying

the strength of  $QQ$  interaction. The strengths of the pairing interaction was fixed through the relation  $G_p = 30/A$  MeV and  $G_n = 20/A$  MeV, which were the same as used by Heestand *et al.* [52] to explain the experimental  $g(2^+)$  data of some even-even Ge, Se, Mo, Ru, Pd, Cd and Te isotopes in Greiner's collective model [53]. For  $^{96}\text{Zr}$ , we have used  $G_n = 22/A$  MeV. The strengths of the pairing interaction fixed for  $^{128,130}\text{Te}$ ,  $^{128,130}\text{Xe}$ ,  $^{150}\text{Nd}$  and  $^{150}\text{Sm}$  were  $G_p = 35/A$  MeV and  $G_n = 35/A$  MeV.

The strengths of the like particle components of the  $QQ$  interaction were taken as:  $\chi_{pp} = \chi_{nn} = 0.0105$  MeV  $b^{-4}$ , where  $b$  is the oscillator parameter. The strength of proton-neutron ( $pn$ ) component of the  $QQ$  interaction  $\chi_{pn}$  was varied so as to obtain the spectra of considered nuclei, namely  $^{94,96}\text{Zr}$ ,  $^{94,96,98,100}\text{Mo}$ ,  $^{98,100,104}\text{Ru}$ ,  $^{104,110}\text{Pd}$ ,  $^{110}\text{Cd}$ ,  $^{128,130}\text{Te}$ ,  $^{128,130}\text{Xe}$ ,  $^{150}\text{Nd}$  and  $^{150}\text{Sm}$  in optimum agreement with the experimental results. The theoretical spectra has been taken to be the optimum one if the excitation energy of the  $2^+$  state  $E_{2^+}$  is reproduced as closely as possible to the experimental value. The prescribed set of parameters for the strength of  $QQ$  interaction are in general different for the initial and final nuclei. They have been tabulated in the previous works describing the  $(\beta^-\beta^-)_{2\nu}$  decay [40, 41], and are consistent with those of Arima suggested on the basis of an empirical analysis of effective two-body interaction [54].

### A. Results of $(\beta^-\beta^-)_{0\nu}$ decay

The phase space factors  $G_{01}$  of  $(\beta^-\beta^-)_{0\nu}$  decay for the  $0^+ \rightarrow 0^+$  transition have been calculated by Doi *et al.* [14] and Boehm and Vogel [18] for  $g_A = 1.25$ . We use the later in our calculations after reevaluating them for  $g_A = 1.254$ . The average energy denominator  $\bar{A}$  is calculated using Haxton's prescription given by  $\bar{A} = 1.12A^{1/2}$  MeV [13]. In Table I, we compile all the required NTMEs  $M_F$ ,  $M_{GT}$ ,  $M_{Fh}$  and  $M_{GT_h}$  for  $^{94,96}\text{Zr}$ ,  $^{98,100}\text{Mo}$ ,  $^{104}\text{Ru}$ ,  $^{110}\text{Pd}$ ,  $^{128,130}\text{Te}$  and  $^{150}\text{Nd}$  nuclei. The four NTMEs are calculated in the approximation of point nucleons, point nucleons plus Jastrow type of SRC, finite size of nucleons with dipole form factor and finite size plus SRC. In the case of point nucleons, the NTMEs  $M_F$  and  $M_{GT}$  are calculated for  $\bar{A}$  and  $\bar{A}/2$  in the energy denominator. It is observed that the NTMEs  $M_F$  and  $M_{GT}$  change by 7.5-10.3 % for  $\bar{A}/2$  in comparison to  $\bar{A}$  in the energy denominator. Hence, the dependence of NTMEs on average excitation energy  $\bar{A}$  is small and the closure approximation is quite good in the case of  $(\beta^-\beta^-)_{0\nu}$  decay as expected. In the approximation of light neutrinos, the NTMEs  $M_F$  and  $M_{GT}$  are reduced by 17-22% and 11.6-14.4% for point nucleon plus SRC and finite size of nucleons respectively. Finally the NTMEs change by 20.8-26.5% with finite size plus SRC. In case of heavy neutrinos, the  $M_{Fh}$  and  $M_{GT_h}$  get reduced by 34.5-39.3% and 65.4-69.5% with the inclusion of finite size and finite size plus SRC.

### B. Limits on effective mass of light and heavy neutrinos

In Table II, we compile the calculated NTMEs  $M_F$ ,  $M_{GT}$ ,  $M_{Fh}$  and  $M_{GT_h}$  of the above mentioned isotopes for the  $0^+ \rightarrow 0^+$  transition in the PHFB as well as other models. Further, we also present the results of shell model [55], QRPA as well as RQRPA calculations by Rodin *et al.* [57], Simkovic *et al.* [56] and pseudo SU(3) [45] for light neutrinos. Besides using different model space, single particle energies and effective two-body interactions, the value of  $g_A$  used in these calculation is different. To be specific,  $g_A = 1.0$  [45],  $g_A = 1.25$  [55, 57, 60] and  $g_A = 1.254$  [17, 56, 58, 59]. The value of  $g_A$  is not available for calculation of Pantis *et al.* [61, 62]. Recently, Simkovic *et al.* [56] have evaluated  $M^{(0\nu)}$  using both QRPA and RQRPA taking an average of 24 calculations. Their smallest and largest NTME  $M^{(0\nu)}$ , calculated in the QRPA(RQRPA) with Jastrow type of correlations, are included in Table II, and for this reason two values are given for each nuclei associated with Ref. [56]. The spreads in NTMEs  $M^{(0\nu)}$  ( $M_N^{(0\nu)}$ ) of light(heavy) neutrinos for  $^{96}\text{Zr}$ ,  $^{100}\text{Mo}$ ,  $^{128,130}\text{Te}$  and  $^{150}\text{Nd}$  isotopes are 6.7(8.5), 127.2(40.1), 5.4(7.0), 2.8(4.2) and 3.9(9.3) respectively. Excluding the result of FQRPA [61], the same spreads turn out to be 2.4(2.1), 4.2(5.8), 2.9(5.9), 2.5(4.2) and 3.9(9.3) respectively. The convergence of the NTMEs calculated in different models to a factor smaller than 4 is encouraging. And it should be taken into account that some calculations do not include deformation effects, and that the size of contribution from the tensorial terms is still being debated and deserves further studies.

We extract the limits on effective light neutrino mass  $\langle m_\nu \rangle$  and heavy neutrino mass  $\langle M_N \rangle$  using the phase space factors evaluated for  $g_A = 1.254$ . However, the NTMEs  $M_F$  and  $M_{Fh}$  need to be evaluated for the same  $g_A$ . We tabulate the extracted limits on effective light neutrino mass  $\langle m_\nu \rangle$  and heavy neutrino mass  $\langle M_N \rangle$  in the same Table II using experimental limits on half-lives  $T_{1/2}^{0\nu}$  given below.

$$\begin{array}{ll}
T_{1/2}^{0\nu} > 1.9 \times 10^{19} \text{ yr } (^{94}\text{Zr}) & [63] & T_{1/2}^{0\nu} > 6.0 \times 10^{17} \text{ yr } (^{110}\text{Pd}) & [66] \\
T_{1/2}^{0\nu} > 1.0 \times 10^{21} \text{ yr } (^{96}\text{Zr}) & [63] & T_{1/2}^{0\nu} > 1.1 \times 10^{23} \text{ yr } (^{128}\text{Te}) & [67] \\
T_{1/2}^{0\nu} > 1.0 \times 10^{14} \text{ yr } (^{98}\text{Mo}) & [64] & T_{1/2}^{0\nu} > 3.0 \times 10^{24} \text{ yr } (^{130}\text{Te}) & [68] \\
T_{1/2}^{0\nu} > 4.6 \times 10^{23} \text{ yr } (^{100}\text{Mo}) & [65] & T_{1/2}^{0\nu} > 1.2 \times 10^{21} \text{ yr } (^{150}\text{Nd}) & [69]
\end{array}$$

No experimental half-life limit on  $(\beta^-\beta^-)_{0\nu}$  decay is available in the case of  $^{104}\text{Ru}$  isotope. In case of  $^{94}\text{Zr}$ ,  $^{98}\text{Mo}$  and  $^{110}\text{Pd}$  isotopes, the observed experimental half-life limits are small and no theoretical calculation has been performed so far. The extracted upper and lower bounds on  $\langle m_\nu \rangle$  and  $\langle M_N \rangle$  from the observed half-life limits  $T_{1/2}^{0\nu}$  using NTMEs calculated in the PHFB model are  $1.40 \times 10^3$  eV,  $3.60 \times 10^6$  eV,  $1.44 \times 10^3$  eV and  $1.05 \times 10^4$  GeV, 3.8 GeV and  $1.01 \times 10^4$  GeV for  $^{94}\text{Zr}$ ,  $^{98}\text{Mo}$  and  $^{110}\text{Pd}$  respectively.

In the case of  $^{96}\text{Zr}$  isotope, the theoretically calculated  $|M^{(0\nu)}|$  in the PHFB model and RQRPA [57] are close. The  $|M^{(0\nu)}|$  calculated in the FQRPA [61] and QPRA [57] are smaller than the presently calculated value by factors of 4.1 and 1.3 respectively while the  $|M^{(0\nu)}|$  calculated in the QRPA [61] is larger by a factor of 1.7. In case of heavy neutrinos, the only available  $|M_N^{(0\nu)}|$  is due to Pantis *et al.* [61]. Using the NTMEs calculated in the PHFB model, the extracted limits on light and heavy neutrino mass from the observed half-life limit  $T_{1/2}^{0\nu} > 1.0 \times 10^{21}$  yr [63] are  $\langle m_\nu \rangle < 45.66$  eV and  $\langle M_N \rangle > 3.4 \times 10^5$  GeV respectively.

The  $(\beta^-\beta^-)_{0\nu}$  decay of  $^{100}\text{Mo}$  is a theoretically well studied case. The NTME  $|M^{(0\nu)}|$  calculated in the PHFB model lies in the range of  $|M^{(0\nu)}|$  calculated in QRPA [57] and close to RQRPA [60]. The NTMEs  $|M^{(0\nu)}|$  calculated in other nuclear models [17, 58, 61, 62] are small in comparison to the NTMEs calculated in the PHFB model. There are six matrix elements available in case of heavy neutrinos. The NTMEs  $|M_N^{(0\nu)}|$  calculated in the QRPA by Tomoda [17] and Hirsch *et al.* [59] are larger by a factor of 1.6 and 3.3 respectively than the present work. All other matrix elements  $|M_N^{(0\nu)}|$  are smaller than the presently calculated value. The extracted upper and lower bounds on light and heavy neutrino masses  $\langle m_\nu \rangle$  and  $\langle M_N \rangle$  from the observed half-life limit  $T_{1/2}^{0\nu} > 4.6 \times 10^{23}$  yr [65] in the PHFB model are 1.08 eV and  $1.32 \times 10^7$  GeV respectively.

The NTME  $|M^{(0\nu)}|$  calculated in the PHFB model and QRPA [17] for  $^{128}\text{Te}$  isotope are close and larger by a factor of 1.8 than the calculated NTME in FQRPA [61]. All other NTMEs  $|M^{(0\nu)}|$  are large in comparison to the result of PHFB model. In case of heavy neutrinos, the NTMEs  $|M_N^{(0\nu)}|$  have been calculated by Tomoda [17], Hirsch *et al.* [59] and Pantis *et al.* [61]. The  $|M_N^{(0\nu)}|$  calculated in our PHFB model is larger than the calculated NTME in FQRPA [61] by a factor of 1.2 and smaller than results of Tomoda [17], Hirsch *et al.* [59] and Pantis *et al.* [61]. The extracted neutrino mass limits using our NTMEs from the observed half-life limit  $T_{1/2}^{0\nu} > 1.1 \times 10^{23}$  yr [67] are  $\langle m_\nu \rangle < 22.05$  eV and  $\langle M_N \rangle > 6.84 \times 10^5$  GeV respectively.

In the case of  $^{130}\text{Te}$  isotope, the  $|M^{(0\nu)}|$  calculated in the PHFB model, SM [55] and QRPA [61] are close. It is smaller than the  $|M^{(0\nu)}|$  calculated in QRPA and its extensions [57, 58, 61]. The presently calculated  $|M^{(0\nu)}|$  is larger by a factor of 1.3 and 1.5 than the calculated values in QPPA [17] and FQRPA [61]. In case of heavy neutrinos, our calculated  $|M_N^{(0\nu)}|$  in the PHFB model is smaller than the available NTMEs  $|M_N^{(0\nu)}|$  calculated in other models. The extracted neutrino mass limits from the observed half-life limit  $T_{1/2}^{0\nu} > 3.0 \times 10^{24}$  yr [68] are  $\langle m_\nu \rangle < 0.63$  eV and  $\langle M_N \rangle > 2.18 \times 10^7$  GeV respectively using NTMEs of the present work.

The NTMEs  $|M^{(0\nu)}|$  have been calculated by Tomoda [17], Hirsch *et al.* [45], Rodin *et al.* [57] and Muto *et al.* [58] for  $^{150}\text{Nd}$  isotope. The  $|M^{(0\nu)}|$  calculated in the PHFB model and pseudo SU(3) [45] are close and smaller by a factor of 3.8 than the  $|M^{(0\nu)}|$  calculated in the QRPA by Muto *et al.* [58]. The  $|M^{(0\nu)}|$  calculated by Rodin *et al.* [57] in QRPA and RQRPA are large in comparison to our calculated results. However, the deformation effect has not been taken into account in the calculation of Rodin *et al.* [57]. Arguably, the results based on the spherical QRPA are larger than ours in the present case as expected. In case of heavy neutrinos, our calculated  $|M_N^{(0\nu)}|$  in the PHFB model is smaller than the reported NTMEs in the QRPA [17, 59]. Using the NTMEs of our PHFB model, the extracted upper and lower bounds on  $\langle m_\nu \rangle$  and  $\langle M_N \rangle$  from the observed half-life limit  $T_{1/2}^{0\nu} > 1.2 \times 10^{21}$  yr [69] are 19.85 eV and  $6.79 \times 10^5$  GeV respectively.

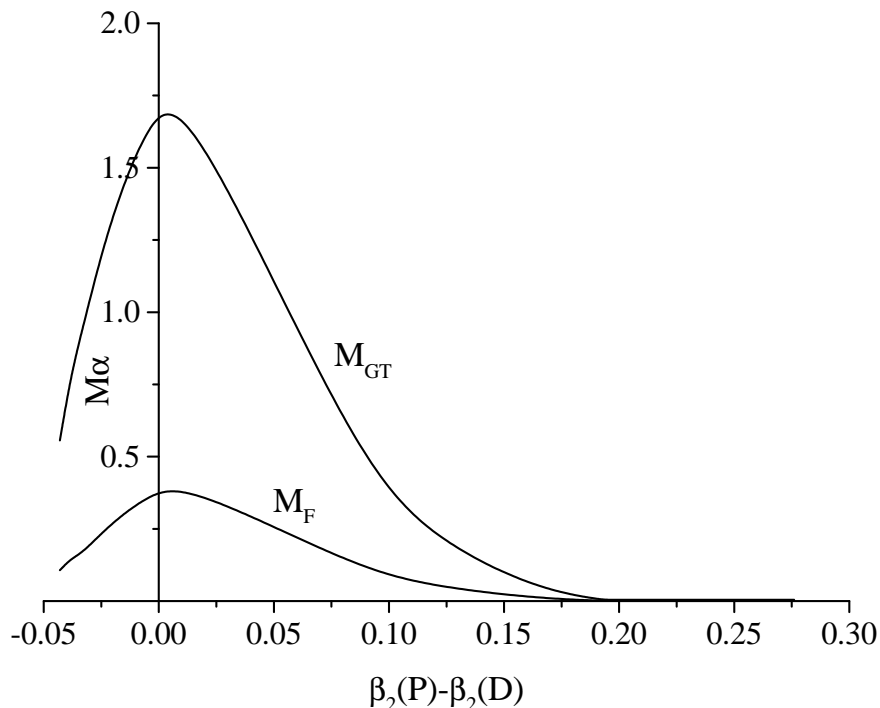


FIG. 1:  $\beta\beta_{0\nu}$  NTME for  $^{150}\text{Nd}$  as a function of the difference in the deformation parameter  $\beta_2$  between the parent and daughter nuclei.

### C. Quadrupolar correlations and deformation

To understand the role of quadrupolar correlations on the NTMEs  $M_\alpha$  ( $\alpha = F, GT, Fh, GTh$ ) of  $(\beta^-\beta^-)_{0\nu}$  decay for the  $0^+ \rightarrow 0^+$  transition, we investigate the variation of the  $M_\alpha$  by changing the strength parameter  $\zeta_{qq}$  of  $QQ$  part of the effective two-body interaction. In Table III, we present the NTMEs  $M_\alpha$  of  $^{94,96}\text{Zr}$ ,  $^{98,100}\text{Mo}$ ,  $^{104}\text{Ru}$ ,  $^{110}\text{Pd}$ ,  $^{128,130}\text{Te}$  and  $^{150}\text{Nd}$  nuclei for different  $\zeta_{qq}$ . In general, it is observed that NTMEs  $M_\alpha$  remain initially almost constant and then start decreasing as the strength parameter  $\zeta_{qq}$  approaches the physical value 1. There are of course few minor observed anomalies which can not be explained at the present stage. This reduction in the magnitude of NTMEs from their maximum values obtained with pure pairing has a clear analogy with their behavior in the presence of particle-particle  $1^+$  proton-neutron correlations [70] which has been widely discussed in the literature (see Ref. [43] and references therein).

To quantify the effect of quadrupolar interaction on  $M_\alpha$ , which is closely related with the nuclear deformation, we define a quantity  $D_\alpha$  as the ratio of  $M_\alpha$  calculated with pure pairing ( $\zeta_{qq} = 0$ ) and with full presence of the quadrupolar interaction ( $\zeta_{qq} = 1$ ). Explicitly, the  $D_\alpha$  is given by

$$D_\alpha = \frac{M_\alpha(\zeta_{qq} = 0)}{M_\alpha(\zeta_{qq} = 1)} \quad (35)$$

The values of  $D_\alpha$  are tabulated in Table IV for the considered nuclei. These values of  $D_\alpha$  suggest that the NTMEs  $M_\alpha$  due to light and heavy neutrino exchange are quenched by factors of 1.92 to 6.25 and 1.92 to 6.27 respectively in the mass region  $94 \leq A \leq 150$  due to the presence of quadrupolar correlations. For comparison, we also give the ratio  $D_{2\nu}$  [40, 41] associated with the same effect in the  $(\beta^-\beta^-)_{2\nu}$  matrix elements, in the last row of the same table, which also change by almost same amount due to the quadrupolar interaction. Hence, it is clear that the deformation effects are important in case of  $(\beta^-\beta^-)_{2\nu}$  as well as  $(\beta^-\beta^-)_{0\nu}$  decay so far as the nuclear structure aspect of  $\beta^-\beta^-$  decay is concerned.

A suppression of the double beta matrix element with respect to the spherical case has been reported when the parent and daughter nuclei have different deformations [71]. To investigate this effect we present in Fig. 1 the NTMEs for  $^{150}\text{Nd}$  as a function of the difference in the deformation parameter  $\beta_2$  between the parent and daughter nuclei. The NTMEs are calculated keeping the deformation for parent nuclei fixed at  $\zeta_{qq}=1$  and the deformation of daughter nuclei are varied by taking  $\zeta_{qq}=0.0$  to 1.5.

It is clear that when the deformations of parent and daughter nuclei are similar the NTMEs have a well defined

maximum, and when the absolute value of the difference in deformation increases the NTMEs are strongly reduced, in full agreement with the results reported in [71]. In the case of  $^{150}\text{Nd}\rightarrow^{150}\text{Sm}$  transition, the large difference in the observed deformation parameters  $\beta_2$  of parent and daughter isotopes suggests that the reduction of NTMEs is substantial. In the present calculation, the magnitude of reduction could be underestimated due to the difference in the theoretically calculated [41] and experimentally observed parametric values of deformations.

#### IV. CONCLUSIONS

The required NTMEs to study  $(\beta^-\beta^-)_{0\nu}$  decay of  $^{94,96}\text{Zr}$ ,  $^{98,100}\text{Mo}$ ,  $^{104}\text{Ru}$ ,  $^{110}\text{Pd}$ ,  $^{128,130}\text{Te}$  and  $^{150}\text{Nd}$  isotopes in mass mechanism are calculated in the PHFB model. It is observed that the NTMEs have a weak dependence on the average excitation energy  $\bar{A}$  of intermediate nucleus and the closure approximation is quite valid, as expected. Further, we extract limits on gauge theoretical parameters, namely  $\langle m_\nu \rangle$  and  $\langle M_N \rangle$  from the available limits on experimental half-lives  $T_{1/2}^{0\nu}$  using NTMEs calculated in the PHFB as well as other models. For the best candidates  $^{100}\text{Mo}$  and  $^{130}\text{Te}$  nuclei, the PHFB, SM [55] and QRPA [61] results are close. Finally, the calculated values of  $D_\alpha$  suggest that the NTMEs  $M_\alpha$  due to light and heavy neutrino exchange are quenched by factors of 1.92 to 6.25 and 1.92 to 6.27 respectively in the mass region  $94 \leq A \leq 150$  due to the deformation. In  $^{150}\text{Nd}$  the difference in deformation between the parent and daughter nuclei is small and adds no extra suppression. We conclude that nuclear structure effects are also important for the  $(\beta^-\beta^-)_{0\nu}$  decay.

This work was partially supported by DST, India vide sanction No. SR/S2/HEP-13/2006, by Conacyt-México and DGAPA-UNAM.

- 
- [1] Y. Ashie *et al.* [Super-Kamiokande Collaboration], Phys. Rev. **D**, **71**, 112005 (2005); Y. Fukuda *et al.* [Super-Kamiokande Collaboration], Phys. Rev. Lett. **82**, 1810 (1999); Phys. Rev. Lett. **82**, 2430 (1999); Phys. Rev. Lett. **82**, 2644 (1999); Phys. Rev. Lett. **81**, 1562 (1998).
  - [2] A. Surdo [Macro Collaboration], Nucl. Phys. Proc. Suppl. **110**, 342 (2002); G. Giacomelli and A. Margiotta, Phys. Atm. Nucl. **67**, 1139 (2004), hep-ex/0407023.
  - [3] M. Sanchez *et al.* [Soudan 2 Collaboration], Phys. Rev. D **68**, 113004 (2003), hep-ex/0307069.
  - [4] B. T. Cleveland *et al.*, Astrophys. **J** **496**, 505 (1998), J. N. Abdurashitov *et al.* [SAGE Collaboration], J. Exp. Theo. Phys. **95**, 181 (2002), astro-ph/0204245; T. Kirsten *et al.* [GALLEX and GNO Collaboration], Nucl. Phys. **B** (Proc. Suppl.) **118**, 33 (2003), C. Cattadori, N. Ferrari and L. Pandola, Nucl. Phys. **B** (Proc. Suppl.) **143**, 3 (2005).
  - [5] S. Fukuda *et al.* [Super-Kamiokande Collaboration], Phys. Lett. **B539**, 179 (2002), hep-ex/0205075; J. Hosaka *et al.* [Super-Kamiokande Collaboration], Phys. Rev. **D** **73**, 112001 (2006).
  - [6] Q. R. Ahmad *et al.* [SNO Collaboration], Phys. Rev. Lett. **89**, 011301 (2002), nucl-ex/0204008, *ibid* **89**, 011302 (2002), nucl-ex/0204009, **87**, 071301 (2001), S. N. Ahmad *et al.*, Phys. Rev. Lett. **90**, 041801 (2003); B. Aharmim *et al.*, Phys. Rev. **C** **72**, 055502 (2005).
  - [7] K. Eguchi *et al.* [KamLand Collaboration], Phys. Rev. Lett. **90**, 021802 (2003), hep-ex/0212021.
  - [8] T. Araki *et al.* [KamLand Collaboration], Phys. Rev. Lett. **94**, 081801 (2005); I. Shimizu, talk at the 10th International Conference on Topics in Astrophysics and Underground Physics, TAUP2007, Sendai, Sept. 11-15, 2007.
  - [9] E. Aliu *et al.* [K2K Collaboration] Phys. Rev. Lett. **94**, 081802 (2005); M. H. Ahn *et al.* [K2K Collaboration], Phys. Rev. Lett. **90**, 041801 (2003), hep-ex/0212007; Phys. Rev. **D74**, 072003 (2006), hep-ex/0606032.
  - [10] D. G. Michael *et al.* [MINOS Collaboration], Phys. Rev. Lett. **97**, 191801 (2006), hep-ex/0708.1495.
  - [11] T. Schwetz, CERN-PH-TH-207, hep-ph/0710.5027.
  - [12] V. I. Tretyak and Y. G. Zdesenko, Atomic data and Nuclear data Tables, **61**, 43 (1995), *ibid* **80**, 83 (2002).
  - [13] W. C. Haxton and G. J. Stephenson, Jr., Prog. Part. Nucl. Phys. **12**, 409 (1984).
  - [14] M. Doi, T. Kotani and E. Takasugi, Prog. Theo. Phys. Suppl. **83**, 1 (1985).
  - [15] J. D. Vergados, Phys. Rep. **133**, 1 (1986); *ibid* **361**, 1 (2002).
  - [16] A. Faessler, Prog. Part. Nucl. Phys. **21**, 183 (1988).
  - [17] T. Tomoda, Rep. Prog. Phys. **54**, 53 (1991).
  - [18] F. Boehm and P. Vogel, Ann. Rev. Nucl. Part. Sci. **34**, 125 (1984); F. Boehm and P. Vogel, Physics of Massive Neutrinos, 2nd ed. (Cambridge University Press, Cambridge 1992).
  - [19] M. Doi and T. Kotani, Prog. Theor. Phys. **89**, 139 (1993).
  - [20] M. K. Moe and P. Vogel, Ann. Rev. Nucl. Part. Sci. **44**, 247 (1994).
  - [21] J. Suhonen and O. Civitarese, Phys. Rep. **300**, 123 (1998).
  - [22] A. Faessler and F. Simkovic, J. Phys. G **24**, 2139 (1998); hep-ph/9901215.
  - [23] H. V. Klapdor (Ed.), Proc. Int. Symp. on Weak and Electromagnetic Interactions in Nuclei, Springer, Berlin, 1986; H. V. Klapdor (Ed.), Neutrinos, Springer, Heidelberg, 1988; H. V. Klapdor and S. Stoica (Ed.), Proc. Int. Workshop on Double

- Beta Decay and Related Topics, Trento, Italy, 1995, World Scientific, Singapore, 1996; H. V. Klapdor-Kleingrothaus, hep-ex/9907040, 9901021 and 9802007; Int. J. Mod. Phys. A **13**, 3953 (1998).
- [24] K. Zuber, Phys. Rep. **305**, 295 (1998).
  - [25] E. Fiorini, Phys. Rep. **307**, 309 (1998).
  - [26] H. Ejiri, Phys. Rep. **338**, 265 (2000).
  - [27] S. R. Elliott and P. Vogel, Ann. Rev. Nucl. Part. Sci. **52**, 115 (2002); hep-ph./0202264.
  - [28] S. R. Elliott and J. Engel, J. Phys. G **30**, R183 (2004); hep-ph/0405078.
  - [29] A. Faessler, Prog. Part. Nucl. Phys. **57**, 162 (2006).
  - [30] F. T. Avignone, Prog. Part. Nucl. Phys. **57**, 170 (2006).
  - [31] P. Vogel, Prog. Part. Nucl. Phys. **57**, 177 (2006).
  - [32] F. Simkovic, Prog. Part. Nucl. Phys. **57**, 185 (2006).
  - [33] H. V. Klapdor-Kleingrothaus *et al.*, Mod. Phys. Lett. A **16**, 2409 (2001); hep-ph/0103062.
  - [34] H. V. Klapdor-Kleingrothaus, I. V. Krivosheina, A. Dietz and O. Chkvorets, Phys. Lett. B **586**, 198 (2004); H. V. Klapdor-Kleingrothaus, A. Dietz, H. L. Harney and I. V. Krivosheina, hep-ph/0201231.
  - [35] C. E. Aalseth *et al.*, Phys. Rev. D **65**, 092007 (2002); hep-ph/0202018.
  - [36] Yu. G. Zdesenko, F. A. Danevich and V. I. Tretyak, Phys. Lett. B **546**, 206 (2002).
  - [37] S. Raman, C. H. Malarkey, W. T. Milner, C. W. Nestor Jr. and P. H. Stelson, Atomic data and Nuclear data Tables **36**, 1 (1987).
  - [38] A. Griffiths and P. Vogel, Phys. Rev. C **46**, 181 (1992).
  - [39] J. Suhonen and O. Civitarese, Phys. Rev. C **49**, 3055 (1994).
  - [40] R. Chandra, J. Singh, P. K. Rath, P. K. Raina and J. G. Hirsch, Eur. Phys. J. A **23**, 223 (2005).
  - [41] S. Singh, R. Chandra, P. K. Rath, P. K. Raina and J. G. Hirsch, Eur. Phys. J. A **33**, 375 (2007).
  - [42] F. Simkovic, G. Pantis, J. D. Vergados and A. Faessler, Phys. Rev. C **60**, 55502 (1999).
  - [43] F. T. Avignone, III, S. R. Elliott, J. Engel, Rev. Mod. Phys. **80**, 481 (2008).
  - [44] J. Suhonen, O. Civitarese, arXiv:0803.1375v1 [nucl-th].
  - [45] J. G. Hirsch, O. Castaños and P. O. Hess, Nucl. Phys. A **582**, 124 (1995).
  - [46] M. Kortalinen and J. Suhonen, nucl-th/0708.0115; M. Kortalinen, O. Civitarese, J. Suhonen and J. Toivanen, Phys. Lett. B **647**, 128 (2007), nucl-th/0701052.
  - [47] H. F. Wu, H. Q. Song, T. T. S. Kuo, W. K. Cheng and D. Strottman, Phys. Lett. B **162**, 227 (1985).
  - [48] N. Onishi and S. Yoshida, Nucl. Phys. A. **395** 19 (1966).
  - [49] B. M. Dixit, P. K. Rath and P. K. Raina, Phys. Rev. C **65**, 034311 (2002); *ibid* C **67**, 059901 (E) (2003).
  - [50] O. Civitarese, A. Faessler, and T. Tomoda, Phys. Lett. B **196**, 11 (1987).
  - [51] M. Baranger and K. Kumar, Nucl. Phys. A **10**, 490 (1968).
  - [52] G. M. Heestand, R. R. Borchers, B. Herskind, L. Grodzins, R. Kalish and D. E. Murnick, Nucl. Phys. A **133**, 310 (1969).
  - [53] W. Greiner, Nucl. Phys. **80**, 417 (1966).
  - [54] A. Arima, Nucl. Phys. A **354**, 19 (1981).
  - [55] E. Caurier, F. Nowacki and A. Poves, Eur. Phys. J. A **36**, 19 (2008), nucl-th/0709.0277.
  - [56] F. Simkovic, A. Faessler, V. Rodin, P. Vogel and J. Engel, Phys. Rev. C **77**, 045503 (2008), nucl-th/0710.2055.
  - [57] V. A. Rodin, A. Faessler, F. Simkovic and P. Vogel, nucl-th/0706.4304; Nucl. Phys. A **766**, 107 (2006).
  - [58] K. Muto, E. Bender and H. V. Klapdor, Z. Phys. A- Atomic Nuclei **334**, 187 (1989).
  - [59] M. Hirsch, H. V. Klapdor-Kleingrothaus and O. Panella, Phys. Lett. B **374**, 7 (1996).
  - [60] F. Simkovic, M. Nowak, W. A. Kaminski, A. A. Raduta and A. Faessler, Phys. Rev. C **64**, 035501 (2001).
  - [61] G. Pantis, F. Simkovic, J. D. Vergados and A. Faessler, Phys. Rev. C **53**, 695 (1996).
  - [62] G. Pantis and J. D. Vergados, Phys. Rep. **242**, 285 (1994).
  - [63] R. Arnold *et al.*, Nucl. Phys. A **658**, 299 (1999).
  - [64] J. H. Fremlin and M. C. Walters, Proc. Phys. Soc. A **65**, 911 (1952).
  - [65] R. Arnold *et al.*, Phys. Rev. Lett. **95**, 182302 (2005).
  - [66] R. G. Winter, Phys. Rev. **85**, 687 (1952).
  - [67] C. Arnaboldi *et al.*, Phys. Lett. B **557**, 167 (2003).
  - [68] C. Arnaboldi *et al.*, hep-ex/0802.3439.
  - [69] A. De Silva, M. K. Moe, M. A. Nelson and M. A. Vient, Phys. Rev. C **56**, 2451 (1997).
  - [70] P. Vogel and M.R. Zirnbauer, Phys. Rev. Lett. **57**, 3148 (1986).
  - [71] R. Alvarez-Rodriguez, P. Sarriguren, E. Moya de Guerra, L. Paceaescu, R. Saakyan, F. Simkovic, Prog. Part. Nucl. Phys. **57**, 251 (2006).

TABLE I: NTMEs  $M_F$ ,  $M_{GT}$ ,  $M_{Fh}$  and  $M_{GT_h}$  for the  $(\beta^-\beta^-)_{0\nu}$  decay of  $^{94,96}\text{Zr}$ ,  $^{98,100}\text{Mo}$ ,  $^{104}\text{Ru}$ ,  $^{110}\text{Pd}$ ,  $^{128,130}\text{Te}$  and  $^{150}\text{Nd}$  isotopes.

Nuclei	NTMEs	Point	Point	Extened	Extended	
		$\bar{A}$	$\bar{A}/2$			+SRC
$^{94}\text{Zr}$	$M_F$	0.4634	0.4983	0.3640	0.3975	0.3433
	$M_{GT}$	-2.2557	-2.4381	-1.7871	-1.9470	-1.6912
	$M_{Fh}$	35.1339		0	21.8092	11.1290
	$M_{GT_h}$	-165.746		0	-101.736	-51.5522
$^{96}\text{Zr}$	$M_F$	0.3494	0.3757	0.2734	0.2991	0.2576
	$M_{GT}$	-1.6264	-1.7614	-1.2681	-1.3923	-1.1958
	$M_{Fh}$	26.7691		0	16.6927	8.5271
	$M_{GT_h}$	-126.284		0	-76.6661	-38.4867
$^{98}\text{Mo}$	$M_F$	0.7951	0.8639	0.6474	0.6960	0.6159
	$M_{GT}$	-3.5921	-3.9033	-2.8955	-3.1293	-2.7502
	$M_{Fh}$	52.1823		0	33.2343	17.2313
	$M_{GT_h}$	-246.172		0	-153.939	-78.8982
$^{100}\text{Mo}$	$M_F$	0.7849	0.8476	0.6339	0.6831	0.6013
	$M_{GT}$	-3.5121	-3.7994	-2.8007	-3.0375	-2.6505
	$M_{Fh}$	53.1825		0	34.3112	17.9096
	$M_{GT_h}$	-250.891		0	-158.446	-81.6304
$^{104}\text{Ru}$	$M_F$	0.6073	0.6582	0.4934	0.5300	0.4684
	$M_{GT}$	-2.5306	-2.7285	-1.9938	-2.1704	-1.8787
	$M_{Fh}$	40.0647		0	26.2356	13.8055
	$M_{GT_h}$	-189.007		0	-120.874	-62.7040
$^{110}\text{Pd}$	$M_F$	0.9020	0.9802	0.7260	0.7835	0.6880
	$M_{GT}$	-4.1660	-4.5419	-3.3365	-3.6125	-3.1611
	$M_{Fh}$	61.9271		0	40.0043	20.8651
	$M_{GT_h}$	-292.144		0	-185.378	-95.6358
$^{128}\text{Te}$	$M_F$	0.4063	0.4460	0.3273	0.3536	0.3107
	$M_{GT}$	-1.7644	-1.9237	-1.3913	-1.5172	-1.3142
	$M_{Fh}$	28.0755		0	17.7056	9.1133
	$M_{GT_h}$	-132.448		0	-82.3872	-42.0190
$^{130}\text{Te}$	$M_F$	0.5252	0.5787	0.4306	0.4616	0.4105
	$M_{GT}$	-2.3468	-2.5723	-1.9001	-2.0472	-1.8055
	$M_{Fh}$	33.6801		0	21.4747	11.1405
	$M_{GT_h}$	-158.887		0	-100.999	-52.2720
$^{150}\text{Nd}$	$M_F$	0.3837	0.4231	0.3182	0.3391	0.3039
	$M_{GT}$	-1.6881	-1.8606	-1.3786	-1.4787	-1.3119
	$M_{Fh}$	23.3705		0	15.3104	8.0695
	$M_{GT_h}$	-110.251		0	-71.4285	-37.3676

TABLE II: Upper and lower bounds on light and heavy neutrino masses  $\langle m_\nu \rangle$  (eV) and  $\langle M_N \rangle$  (GeV) respectively for the  $(\beta^-\beta^-)_{0\nu}$  decay of  $^{94,96}\text{Zr}$ ,  $^{98,100}\text{Mo}$ ,  $^{110}\text{Pd}$ ,  $^{128,130}\text{Te}$  and  $^{150}\text{Nd}$  isotopes in different nuclear models.

Nuclei	Model	Ref.	$M_F$	$M_{GT}$	$M^{(0\nu)}$	$\langle m_\nu \rangle$	$M_{Fh}$	$M_{GT_h}$	$M_N^{(0\nu)}$	$\langle M_N \rangle$
$^{94}\text{Zr}$	PHFB	*	0.3433	-1.6912	2.0345	$1.40 \times 10^3$	11.1290	-51.5522	62.6812	$1.05 \times 10^4$
$^{96}\text{Zr}$	PHFB	*	0.2576	-1.1958	1.4534	45.66	8.5271	-38.4867	47.0138	$3.40 \times 10^5$
	QRPA	[61]	-0.312	2.097	2.409	27.55			99.062	$7.16 \times 10^5$
	FQRPA	[61]	0.639	0.280	0.359	184.8			11.659	$8.42 \times 10^4$
	RQRPA	[57]			$1.20^{+0.14}_{-0.14}$	55.30				
	QRPA	[57]			$1.12^{+0.03}_{-0.03}$	59.25				
	RQRPA	[56]			1.01	65.70				
	RQRPA	[56]			1.31	50.65				
	QRPA	[56]			1.34	49.52				
	QRPA	[56]			1.79	37.07				
$^{98}\text{Mo}$	PHFB	*	0.6159	-2.7502	3.3661	$3.60 \times 10^6$	17.2313	-78.8982	96.1295	3.8
$^{100}\text{Mo}$	PHFB	*	0.6013	-2.6505	3.2518	1.08	17.9096	-81.6304	99.5400	$1.32 \times 10^7$
	QRPA	[58, 59]	-1.356	0.763	2.119	1.65	-64.0	269.0	333.0	$4.56 \times 10^7$
	QRPA	[17]	-0.588	1.76	2.348	1.49	-29.141	126.819	155.960	$2.14 \times 10^7$
	QRPA	[62]	0.272	2.86	2.588	1.35			56.914	$7.80 \times 10^6$
	QRPA	[61]	-0.471	0.615	1.086	3.22			76.752	$1.05 \times 10^7$
	FQRPA	[61]	-0.548	-0.584	0.036	97.16			8.304	$1.14 \times 10^6$
	RQRPA	[60]	-0.819	2.620	3.439	1.02	-28.352	34.200	62.552	$8.57 \times 10^6$
	RQRPA	[57]			$2.78^{+0.19}_{-0.19}$	1.26				
	QRPA	[57]			$3.34^{+0.19}_{-0.19}$	1.05				
	RQRPA	[56]			2.22	1.58				
	RQRPA	[56]			2.77	1.26				
	QRPA	[56]			3.53	0.99				
	QRPA	[56]			4.58	0.76				
$^{110}\text{Pd}$	PHFB	*	0.6880	-3.1611	3.8491	$1.44 \times 10^3$	20.8651	-95.6358	116.5009	$1.01 \times 10^4$
$^{128}\text{Te}$	PHFB	*	0.3107	-1.3142	1.6249	22.05	9.1133	-42.0190	51.1323	$6.84 \times 10^5$
	QRPA	[58, 59]	-1.184	3.103	4.287	8.36	-55.0	248.0	303.0	$4.05 \times 10^6$
	QRPA	[17]	-0.440	1.488	1.928	18.58	-22.200	100.469	122.669	$1.64 \times 10^6$
	QRPA	[61]	-0.044	2.437	2.480	14.45			101.233	$1.35 \times 10^6$
	FQRPA	[61]	0.391	1.270	0.879	40.76			43.205	$5.78 \times 10^5$
	SM	[55]	-0.31	2.36	2.67	13.42				
	RQRPA	[57]			$3.23^{+0.12}_{-0.12}$	11.09				
	QRPA	[57]			$3.64^{+0.13}_{-0.13}$	9.84				
	RQRPA	[56]			2.46	14.56				
	RQRPA	[56]			3.06	11.71				
	QRPA	[56]			3.77	9.50				
	QRPA	[56]			4.76	7.53				
	$^{130}\text{Te}$	PHFB	*	0.4105	-1.8055	2.2160	0.63	11.1405	-52.2720	63.4125
QRPA		[58, 59]	-0.977	2.493	3.470	0.40	-48.0	219.0	267.0	$9.19 \times 10^7$
QRPA		[17]	-0.385	1.289	1.674	0.83	-19.582	88.576	108.158	$3.73 \times 10^7$
QRPA		[61]	-0.009	2.327	2.336	0.60			92.661	$3.19 \times 10^7$
FQRPA		[61]	0.337	1.833	1.496	0.93			102.135	$3.51 \times 10^7$
SM		[55]	-0.28	2.13	2.41	0.58				
RQRPA		[57]			$2.95^{+0.12}_{-0.12}$	0.47				
QRPA		[57]			$3.26^{+0.12}_{-0.12}$	0.43				
RQRPA		[56]			2.27	0.61				
RQRPA		[56]			2.84	0.49				
QRPA		[56]			3.38	0.41				
QRPA		[56]			4.26	0.33				
$^{150}\text{Nd}$		PHFB	*	0.3039	-1.3119	1.6158	19.85	8.0695	-37.3676	45.4371
	QRPA	[58, 59]	-1.821	4.254	6.075	5.28	-78.0	344.0	422.0	$6.31 \times 10^6$
	QRPA	[17]	-0.629	1.989	2.618	12.25	-28.385	124.700	153.085	$2.29 \times 10^6$
	pSU(3)	[45]			1.570	20.43				
	RQRPA	[57]			$4.16^{+0.16}_{-0.16}$	7.71				
	QRPA	[57]			$4.75^{+0.20}_{-0.20}$	6.77				

TABLE III: Effect of variation in  $\zeta_{qq}$  on NTMEs  $M_\alpha$  ( $\alpha = F, GT, Fh$  and  $GTh$ ) of  $(\beta^- \beta^-)_{0\nu}$  decay.

$\zeta_{qq}$		0.00	0.20	0.40	0.60	0.80	0.90	0.95	1.00	1.05	1.10	1.20	1.30	1.40	1.50
$^{94}\text{Zr}$	$ M_F $	0.9525	0.9138	0.9332	0.9325	0.8380	0.3889	0.3450	0.3433	0.3118	0.2755	0.0716	0.0777	0.0419	0.1962
	$ M_{GT} $	4.1580	4.0673	4.1432	4.1588	3.8157	1.8974	1.6863	1.6912	1.5779	1.4556	0.3196	0.3535	0.2095	1.0231
	$ M_{Fh} $	26.4106	25.7395	26.1951	26.2492	24.1958	12.3099	11.0816	11.1290	10.3310	9.3615	2.5563	2.8608	1.9605	6.1134
	$ M_{GTh} $	120.702	118.031	120.066	120.406	111.251	56.9742	51.1542	51.5522	47.9816	43.6137	11.4948	12.8413	8.8149	27.9369
$^{96}\text{Zr}$	$ M_F $	1.2254	1.2627	1.2513	1.2397	0.9641	0.6311	0.4358	0.2576	0.1347	0.0773	0.0302	0.0772	0.0730	0.0624
	$ M_{GT} $	5.3171	5.4406	5.4482	5.4491	4.4492	3.0011	2.0655	1.1958	0.6002	0.3336	0.1201	0.3148	0.3050	0.2669
	$ M_{Fh} $	33.4814	34.2490	34.2199	34.1506	28.0203	19.4408	13.8870	8.5271	4.5763	2.6647	1.0640	2.5368	2.5209	2.2641
	$ M_{GTh} $	152.749	156.080	156.213	156.145	128.921	89.3919	63.4324	38.4867	20.3309	11.7475	4.6909	11.1870	11.1178	9.9883
$^{98}\text{Mo}$	$ M_F $	1.2471	1.2890	1.3440	1.2762	0.5080	0.2813	0.6198	0.6159	0.1425	0.0799	0.0420	0.0478	0.1829	0.1325
	$ M_{GT} $	5.2875	5.4677	5.6704	5.4994	2.3544	1.3173	2.8606	2.7502	0.5978	0.3480	0.1970	0.2278	0.8807	0.6494
	$ M_{Fh} $	33.4621	34.5055	35.7334	34.6749	15.6358	9.1876	18.2205	17.2313	4.3304	2.4780	1.2824	1.4689	5.2861	3.9076
	$ M_{GTh} $	151.618	156.392	161.819	157.628	71.7167	42.0018	83.7605	78.8982	19.4513	11.3293	6.1742	7.1270	25.2409	19.1005
$^{100}\text{Mo}$	$ M_F $	1.2780	1.4364	1.4561	1.5051	1.5178	0.6441	0.8557	0.6013	0.3241	0.2992	0.3380	0.4183	0.1560	0.1741
	$ M_{GT} $	5.7255	6.2099	6.3320	6.5392	6.6479	3.0258	3.9287	2.6505	1.3574	1.2403	1.3153	1.6460	0.7130	0.7717
	$ M_{Fh} $	35.3409	38.4610	39.1496	40.3860	40.9767	19.6010	25.4105	17.9096	9.5889	8.9123	9.5424	11.3697	4.4923	4.6833
	$ M_{GTh} $	161.769	174.981	178.291	183.884	186.830	90.2545	116.663	81.6304	43.7223	40.4320	42.7095	50.5883	21.3888	21.5911
$^{104}\text{Ru}$	$ M_F $	1.6121	1.5740	1.5482	1.5771	0.6685	0.6570	0.5946	0.4684	0.3277	0.2351	0.1826	0.0241	0.1693	0.1667
	$ M_{GT} $	7.3361	7.2600	7.2490	7.3978	3.0294	2.8126	2.4618	1.8787	1.2527	0.8447	0.6502	0.0810	0.3864	0.3802
	$ M_{Fh} $	43.9292	43.4102	43.2413	44.1136	19.5841	19.3482	17.4213	13.8055	9.6922	6.7778	5.2601	0.6816	3.8479	3.7724
	$ M_{GTh} $	201.252	199.327	199.057	203.139	90.9183	88.5215	79.2869	62.7040	43.9749	30.8020	23.8972	2.9638	14.0488	13.7353
$^{110}\text{Pd}$	$ M_F $	1.7381	1.7238	1.7485	1.7469	1.3849	0.9328	0.7303	0.6880	0.5537	0.3456	0.2808	0.1851	0.1458	0.1118
	$ M_{GT} $	8.4105	8.3851	8.4792	8.4913	6.5005	4.2640	3.3472	3.1611	2.6277	1.7438	1.3719	0.8580	0.6526	0.5252
	$ M_{Fh} $	49.0177	48.8272	49.4187	49.4697	40.1148	28.3224	22.6514	20.8651	16.2553	10.5955	8.4977	5.4096	4.3595	3.6178
	$ M_{GTh} $	225.933	225.220	227.828	228.150	185.198	129.798	103.531	95.6358	75.4985	49.9589	40.3671	26.0640	21.4753	18.2737
$^{128}\text{Te}$	$ M_F $	1.3400	1.3207	1.3410	0.6911	0.3791	0.3318	0.3096	0.3107	0.2643	0.2165	0.0207	0.0033	0.0002 <sup>†</sup>	0.0004
	$ M_{GT} $	5.8530	5.7535	5.8369	3.1351	1.6661	1.4220	1.3133	1.3142	1.1136	0.9261	0.0962	0.0147	0.0008 <sup>†</sup>	0.0015
	$ M_{Fh} $	35.4843	35.3388	35.8018	18.7882	10.7613	9.6002	9.0907	9.1133	8.0909	6.8243	0.7938	0.1577	0.0138 <sup>†</sup>	0.0249
	$ M_{GTh} $	166.140	165.460	167.632	88.4856	50.3124	44.4687	41.9310	42.0190	37.2069	31.6283	3.9705	0.7864	0.0680 <sup>†</sup>	0.1220
$^{130}\text{Te}$	$ M_F $	1.2162	1.2339	1.2371	1.1357	0.5663	0.5283	0.4628	0.4105	0.3690	0.3610	0.3206	0.2697	0.2570	0.1062
	$ M_{GT} $	5.3383	5.4108	5.4179	5.0086	2.5392	2.3577	2.0562	1.8055	1.6091	1.5650	1.3646	1.1307	1.0735	0.4562
	$ M_{Fh} $	32.4773	32.9039	33.0896	30.4365	14.9999	14.1131	12.5245	11.1405	10.1820	9.9612	8.8699	7.7887	7.4791	3.3935
	$ M_{GTh} $	151.956	153.963	154.832	142.316	70.4659	66.3531	58.8479	52.2720	47.6396	46.5332	41.2186	35.9060	34.4146	15.8394
$^{150}\text{Nd}$	$ M_F $	1.7574	1.7866	1.7941	1.7618	1.1265	0.8929	0.4816	0.3039	0.2466	0.2087	0.1809	0.1258	0.1226	0.0981
	$ M_{GT} $	8.1997	8.3249	8.3573	8.1859	5.2625	4.1539	2.1505	1.3119	1.0927	0.9657	0.9218	0.7280	0.6640	0.5203
	$ M_{Fh} $	49.9349	50.7036	50.9731	50.0155	31.8413	24.7475	13.0967	8.0695	6.5722	5.6055	5.2347	4.0764	3.9110	3.2948
	$ M_{GTh} $	234.218	237.784	238.980	234.268	149.171	116.206	61.0345	37.3676	30.6928	26.4558	25.3258	20.5210	19.8597	17.1640

<sup>†</sup>denotes  $\zeta_{qq} = 1.41$ .

TABLE IV: Ratios  $D_\alpha$  for  $^{94,96}\text{Zr}$ ,  $^{98,100}\text{Mo}$ ,  $^{104}\text{Ru}$ ,  $^{110}\text{Pd}$ ,  $^{128,130}\text{Te}$  and  $^{150}\text{Nd}$  isotopes.

Ratios	$^{94}\text{Zr}$	$^{96}\text{Zr}$	$^{98}\text{Mo}$	$^{100}\text{Mo}$	$^{104}\text{Ru}$	$^{110}\text{Pd}$	$^{128}\text{Te}$	$^{130}\text{Te}$	$^{150}\text{Nd}$
$D_F$	2.77	4.76	2.02	2.13	3.44	2.53	4.31	2.96	5.78
$D_{GT}$	2.46	4.45	1.92	2.16	3.90	2.66	4.45	2.96	6.25
$D_{Fh}$	2.37	3.93	1.94	1.97	3.18	2.35	3.89	2.92	6.19
$D_{GTh}$	2.34	3.97	1.92	1.98	3.21	2.36	3.95	2.91	6.27
$D_{2\nu}$	2.29	3.70	1.86	2.33	5.47	3.14	4.26	2.89	5.94